Long-Term Carotid Plaque Progression and the Role of Intraplaque Hemorrhage: Analysis from Deep Learning-based Longitudinal Vessel Wall Imaging

Yin Guo MS[1], Ebru Yaman Akcicek MD[2], Daniel S. Hippe MS[3], SeyyedKazem HashemizadehKolowri PhD[2], Xin Wang BS[4], Halit Akcicek MD[2], Gador Canton PhD[5], Niranjan Balu PhD[5], Duygu Baylam Geleri MD[5], Taewon Kim MD[5,6], Dean Shibata MD[5], Kaiyu Zhang BS[1], Xiaodong Ma PhD[2], Marina S. Ferguson MS[5], Mahmud Mossa-Basha MD[5], Thomas S. Hatsukami MD[7] and Chun Yuan PhD[1,2,5]

[1]Department of Bioengineering, University of Washington, Seattle, WA, USA
[2]Department of Radiology and Imaging Science, University of Utah School of Medicine, Salt Lake City, UT, USA
[3]Clinical Biostatistics, Clinical Research Division, Fred Hutchinson Cancer Center, Seattle, WA, USA
[4]Department of Electrical and Computer Engineering, University of Washington, Seattle, WA, USA
[5]Department of Radiology, University of Washington School of Medicine, Seattle, WA, USA
[6]Department of Neurology, Incheon St. Mary's Hospital, College of Medicine, The Catholic University of Korea, Seoul, Korea
[7]Department of Surgery, University of Washington School of Medicine, Seattle, WA, USA

Address for correspondence:
Chun Yuan, PhD
850 Republican St, Rm 124
Seattle, WA 98109
Email: cyuan@uw.edu
Phone: 206-616-9346

Funding disclosure: This study was funded by National Institutes of Health under grant R01-HL103609, R01-NS125635 and R01-NS127317.

Running title: Deep learning-based plaque progression and IPH analysis
Word count: 3850

Abstract

Background: Carotid atherosclerosis is a major etiology of stroke. Although intraplaque hemorrhage (IPH) is known to increase stroke risk and plaque burden, its long-term effects on plaque dynamics remain unclear.
Objectives: This study aimed to evaluate the long-term impact of IPH on carotid plaque burden progression using deep learning-based segmentation on multi-contrast vessel wall imaging (VWI).
Methods: Twenty-eight asymptomatic subjects with carotid atherosclerosis underwent an average of 4.7 ± 0.6 VWI scans over 5.8 ± 1.1 years. Deep learning pipelines segmented the carotid vessel walls and IPH. Bilateral plaque progression was analyzed using generalized estimating equations, and linear mixed-effects models evaluated long-term associations between IPH occurrence, IPH volume (%HV), and plaque burden (%WV) progression.
Results: Two subjects with ipsilateral IPH developed new ischemic infarcts during follow-up. IPH was detected in 23/50 of arteries. Of arteries without IPH at baseline, 11/39 developed new IPH that persisted, while 5/11 arteries with baseline IPH exhibited it throughout the study. Bilateral plaque growth was significantly correlated ($r = 0.54$, $p < 0.001$), but this symmetry was weakened with IPH presence. The progression rate for arteries without IPH was -0.001 %/year ($p = 0.895$). However, IPH presence or development at any point was associated with a 2.34% absolute increase in %WV ($p < 0.001$), and %HV was associated with 0.73% per 2-fold increase over the mean of %HV ($p = 0.005$).
Conclusions: IPH may persist asymptomatically for extended periods. While arteries without IPH demonstrated minimal progression under contemporary treatment, IPH significantly accelerated long-term plaque growth.

Key words: Stroke, Carotid atherosclerosis, Intraplaque hemorrhage, Vessel wall MRI, Deep learning

Abbreviations list:
IPH: intraplaque hemorrhage
VWI: vessel wall magnetic resonance imaging
CEA: carotid endarterectomy
MERGE: motion-sensitized driven equilibrium prepared rapid gradient echo
SNAP: simultaneous non-contrast angiography and intraplaque hemorrhage imaging
%WV: percent wall volume
%HV: percent hemorrhage volume

Introduction

Stroke remains the fifth leading cause of mortality in the United States, with an 8.4% increase in the age-adjusted death rate from 2011 to 2021[1]. Carotid atherosclerosis is a leading etiology in stroke[2]. The progression of carotid atheroma, which leads to a reduction in vessel lumen and eventual plaque rupture, is closely related to the risk of cerebrovascular ischemic events[3,4]. Understanding the mechanisms driving plaque evolution is essential for improving stroke prevention strategies.

A recent meta-analysis demonstrated the prevalence of intraplaque hemorrhage (IPH) in patients with both symptomatic and asymptomatic carotid stenosis and identified IPH as a stronger predictor of stroke than any known clinical risk factors[5]. Moreover, IPH is associated with increasing lumen stenosis and rapid vessel wall growth[6–9]. Despite this, little is known about the long-term behavior of IPH, including its occurrence, resolution, and distribution over extended periods, as most studies have been limited to follow-ups of one to two years[7–9]. Its long-term impact on plaque progression also remains inadequately explored[6].

Traditionally, manual analysis of longitudinal vessel wall imaging MRI (VWI) has limited the ability to study carotid atherosclerosis due to its labor-intensive and expertise-dependent nature. Advances in deep learning-based segmentation now enabled automated, reproducible measurements of the carotid vessel wall[10–12] and IPH, facilitating comprehensive studies of plaque dynamics over longer follow-up periods.

This study leverages these tools to analyze carotid atherosclerosis in an asymptomatic cohort over approximately six years. By investigating both systemic and localized trends in plaque evolution, this work provides novel insights into the natural history of carotid atherosclerosis,

emphasizing the critical role of IPH in driving plaque burden progression and its implications for stroke prevention.

Methods

Study population

Participants for this study were recruited as part of a prospective cohort study over a ten-year period (2012-2022), aimed at examining the natural history of carotid atherosclerosis through serial VWI. Eligible participants included patients aged 35 years and older with clinically identified atherosclerosis in at least one carotid artery and without cerebrovascular events in the six months prior to enrollment. Study procedures and consent forms were reviewed and approved by the institutional review board, and all participants provided written informed consent prior to enrollment. Detailed information on cohort recruitment has previously been published[9].

To monitor the evolution of atherosclerotic plaque, serial VWI scans with consistent parameters (detailed below) were conducted up to five times during the study period. For the analysis of the long-term plaque burden progression and the effects of IPH, we conducted a retrospective analysis of a subset of participants. Inclusion criteria for this retrospective analysis required subjects to have undergone at least three VWIs over a minimum span of five years. Arteries with a history of carotid endarterectomy (CEA) or stenting at study entry were excluded. Scans of arteries performed after CEA or stenting were also excluded.

MR Imaging Protocol

Two large-coverage three-dimensional isotropic VWI sequences were performed using a 3.0T Philips Ingenia CX scanner (Philips Healthcare, Best, The Netherlands): 1) Motion-sensitized driven equilibrium prepared rapid gradient echo sequence (MERGE[13]) was used to delineate vessel wall morphology; 2) an inversion-recovery gradient echo sequence with phase-sensitive reconstruction (simultaneous non-contrast angiography and intraplaque hemorrhage imaging,

SNAP[14]) was used to detect and measure IPH. Detailed description of both sequences and imaging parameters can be found elsewhere[9,15].

Ischemic infarcts assessment

Conventional brain MRI examinations, including diffusion weighted imaging (DWI), susceptibility weighted imaging (SWI), and T2-fluid attenuated inversion recovery (FLAIR), were performed at all VWI time points. A board-certified neuroradiologist directly compared the baseline and follow-up brain MRI images and scored for any incident infarcts (FLAIR and DWI images) or hemorrhages (SWI images). Vascular territory and signs of acuity or associated hemorrhage were noted for the infarcts.

Deep Learning-based Vessel Wall and IPH segmentation

Two deep learning-based imaging analysis pipelines were developed to bilaterally segment the carotid vessel wall and IPH on MERGE and SNAP sequences, respectively. Each scan was segmented independently.

For the segmentation of carotid lumen and outer wall boundary using MERGE[16], the location of the left and right common carotid bifurcations was identified automatically. On each side, a 3D bounding box encompassing the bifurcation area as well as the distal and proximal segments of the bifurcation was extracted and then used for a preliminary 3D lumen segmentation. A trained radiologist reviewed the preliminary segmentation to assess image quality and ensure that the lumen from all slices encompassing the bifurcation region were correctly localized. Finally, 2D patches along both carotids were segmented slice-by-slice using a 2.5D convolutional neural network.

To segment IPH from SNAP, a nnUNet[17]-based algorithm was trained to identify hyperintense signals on the 2D axial reformatted images (with 2mm spacing) surrounding the bilateral bifurcations.

Detailed information about the training dataset and extensive validation studies can be found in the supplementary materials. The external validation datasets encompass histological validation of IPH detection and scan-rescan reproducibility assessments of both vessel wall and IPH segmentation.

For each MERGE image, after obtaining lumen and outer wall segmentations of the same artery, the range of slices with wall thickness greater than 2mm in any scan was included as atherosclerotic plaque. Plaque burden was defined as the percent wall volume (%WV), calculated as wall volume divided by total vessel volume, multiplied by 100.

For each SNAP image per artery per time point, IPH was categorized as present (IPH+) or absent (IPH-). IPH volume was aggregated as the sum of IPH areas per slice multiplied by 2mm, and percent hemorrhage volume (%HV) was defined as IPH volume divided by wall volume, multiplied by 100.

Statistical Analysis

Summary statistics of baseline demographics are presented as mean ± standard deviations (SDs) for continuous variables and counts with percentage for categorical variables.

For each analyzable plaque, a linear model was fitted across all available time points to determine the long-term growth rate of plaque burden[18], defined as annualized absolute change in %WV, expressed in units of percent per year. The method for deriving the long-term plaque growth rate is illustrated in Supplementary Figure 1. Generalized estimating equation (GEE)-

based linear regression models were used to evaluate associations of the long-term growth rate of each side with the contralateral side, adjusted for potential confounding factors of age, sex and statin use. Effect sizes were summarized using the partial correlation coefficient.

In all arteries, to investigate whether long-term progression rate in plaque burden depends on presence and volume of IPH, we employed a linear mixed-effects model. This model used %WV as the primary outcome variable and included random intercepts to account for within-subject and within-artery correlation. As fixed effects, the model included time as a continuous variable to estimate the growth rate of %WV and account for variation in scan intervals, a binary predictor indicating IPH presence, and %HV to assess the effect of IPH volume. %HV was log2-transformed to reduce right skewness, and further transformed such that it equals zero when IPH is absent, and equals the deviation from the population mean when IPH is present. The model setup was designed to disentangle the effects of the presence and volume of IPH on plaque burden progression. This model was further adjusted for age, sex and statin use.

All statistical analyses were performed using R 4.4.0. A two-sided p-value < 0.05 was considered statistically significant.

Results

Patient Characteristics

A total of 98 subjects were recruited prospectively, and population demographics can be found in the referenced publication[9]. Among these, 28 subjects underwent at least three VWIs over a span of at least five years and were therefore included in this retrospective analysis. All subjects were under contemporary medical management, and the baseline clinical information of these 28 subjects is presented in Table 1. After three scans were excluded due to poor image quality, each subject had an average of 4.7 ± 0.6 scans within 5.8 ± 1.1 years. Supplementary Figure 2 shows the study flow chart.

Among the 56 carotid arteries within the 28 subjects, six were excluded due to prior history of CEA or having fewer than three available scans due to CEA during the study period. The remaining 50 arteries from 28 subjects were included in artery-level analyses. Of these subjects, there were 22 with bilateral arteries available (44 arteries) for the subject-level analysis where plaque growth on each side was compared.

IPH Presence, Occurrences, and Relation to New Infarcts

Among the 50 carotid arteries from 28 subjects, 23 arteries (46%) from 17 subjects (60.7%) showed presence of IPH on VWI at any time point during the study period. Of the 39 IPH- arteries at the baseline scan, eleven (28.2%) became IPH+ on all subsequent scans after the initial occurrence of IPH, and one artery (2.56%) developed new IPH on the second scan but reverted to IPH- on scans 3 to 5. Of the 11 arteries that were IPH+ at baseline, IPH persisted in five (45.5%) throughout the study, whereas six (54.5%) demonstrated resolution of IPH before the final scan.

During the follow-up, three subjects (10.7%) developed new ischemic infarcts. Of these, one subject had no detectable IPH in either carotid artery at any time point. Another subject consistently exhibited ipsilateral IPH+ and contralateral IPH- across all scans. In the third subject, a new infarct was detected at the third scan, coinciding with the appearance of new ipsilateral IPH. Subsequently, the contralateral side transitioned from IPH- to IPH+ at the fourth scan. Overall, two new infarcts occurred among the 17 subjects with either unilateral or bilateral IPH.

Bilateral Symmetry in Plaque Evolution and the Disruptive Role of IPH

In the 22 subjects with bilateral analyzable arteries, the average %WV growth rate was -0.19 ± 0.74 %/year for the left carotid artery and 0.04 ± 0.54 %/year for the right. The long-term plaque growth rate of one side was moderately correlated ($r = 0.54$, $p < 0.001$) with the contralateral side. The significant correlation remained after adjusting for age, sex and statin use ($r = 0.43$, $p = 0.005$). Figure 1 provides an example of bilateral plaque burden increases over five scans. The association between plaque progression on the left and right sides is visualized in Figure 2.

The 22 subjects were further divided into two sub-groups based on the presence of IPH. In nine subjects, IPH was not detected at any time point, while 13 subjects had either unilateral or bilateral IPH during the study period. Within the IPH- subgroup, significant associations of plaque progression between one side and its contralateral part were found ($r = 0.57$, $p < 0.001$). However, in the group with IPH present, the correlation coefficient decreased, and the association no longer remained significant ($r = 0.28$, $p = 0.187$). This suggests that the presence of IPH disrupts the systemic, symmetric trend of bilateral plaque evolution. The correlation of bilateral long-term plaque progression in the two subgroups is visualized in Figure 2.

IPH's Long-term Impact on Plaque Progression

Building on these findings, we further evaluated both the presence and the volume of IPH on %WV progression using a linear mixed-effects model. In the unadjusted model, the random effects for patients and arteries accounted for individual variability, with SDs of 4.3% and 1.89%, respectively. The SD of the residual term is 3.08%. This suggests considerable variability in %WV progression among patients and between bilateral arteries within the same patient. The progression of %WV over time in arteries without IPH was minimal, with an average rate of -0.001 %/year ($p = 0.895$). However, the presence and occurrence of IPH at any point was a significant predictor, associated with a 2.34% absolute increase in %WV ($p < 0.001$). This indicates that patients with IPH had higher %WV compared to those without IPH and that the development of new IPH was significantly associated with an increase in plaque burden. Furthermore, %HV was significantly associated with %WV, with a coefficient of 0.73 ($p = 0.005$). This means that a 1-unit increase in the log2-transformed %HV, equivalent to a doubling of the mean of %HV, resulted in a 0.73% absolute increase in %WV. These findings highlight the significant impact of both the presence and volume of IPH on the progression of carotid plaque burden over time, as illustrated in Figure 3. Figure 4 provides an example of plaque progression over four scans, highlighting the increasing plaque burden alongside the occurrence (scan 3) and subsequent volume expansion (scan 4) of IPH.

When adjusted for age, sex, and statin use, the linear mixed-effects model continued to show strong associations between IPH and %WV progression. The presence of IPH was associated with an adjusted 2.29% absolute increase in %WV ($p < 0.001$), and the %HV association

persisted, with a coefficient of 0.74% (p = 0.004), similar to the unadjusted model. Age, sex, and statin use had minimal impact on %WV progression (p = 0.321, 0.568, and 0.710, respectively).

Discussion

By leveraging two deep learning-based segmentation pipelines on two large-coverage 3D MR vessel wall imaging (VWI) sequences, we comprehensively evaluated carotid plaque features across an average of five scans over six years in an asymptomatic patient cohort. The role of intraplaque hemorrhage (IPH) in long-term plaque progression can be characterized in two critical ways. First, while plaque progression on one side was significantly correlated with the contralateral side, reflecting the systemic nature of atherosclerotic disease, this symmetry was notably weakened in subjects with IPH, suggesting a more localized effect. Second, despite contemporary medical management, the occurrence and volume of IPH were strongly associated with plaque burden increase, whereas plaques without IPH remained stable over the study period. These findings deepen our understanding of the long-term and pivotal role IPH plays in the natural history of carotid atherosclerosis and underscore the importance of early IPH detection for optimized strategies in managing atherosclerosis.

Previous studies have demonstrated carotid plaque symmetry by comparing cross-sectional measurements of plaque burden between bilateral carotid arteries, as observed in ex vivo imaging studies[19] and in vivo assessments using ultrasound[20] and VWI[21]. Our study extends this understanding with longitudinal follow-up over a six-year period, which reveals not just static morphological symmetry but also symmetrical trends in bilateral plaque progression. Our results suggest that in patients with bilateral disease, monitoring the more advanced plaque could offer valuable prognostic insights into the less advanced contralateral plaque, as signs of progression in the more advanced plaque may indicate elevated bilateral risk.

Notably, as demonstrated by Li et al.[21], IPH exhibits low concordance between left and right carotid plaques, with unilateral or bilateral IPH frequently reported in the current and other

studies, underscoring the role of localized factors in its pathogenesis. Studies showed that IPH development, likely driven by the rupture of neo-vessels, is shaped by conditions such as hemodynamic forces[22], calcification[9], and inflammation[23] within the plaque microenvironment. At the same time, systemic factors still significantly contribute to the development of IPH. For instance, the Rotterdam Study[24], in a cross-sectional analysis, identified pulse pressure as the most significant predictor of IPH, independent of plaque burden and other cardiovascular risk factors. Similarly, another longitudinal study associated male sex and hypertension with an increase in IPH[9]. Understanding the interplay between these localized and systemic influences is critical for advancing our understanding of pathophysiology of IPH development and its impact on plaque stability.

IPH is a dynamic process with the potential for growth or resolution over time. Longitudinal follow-up studies have shown that its hyperintense signal on VWI, likely attributable to methemoglobin from hemoglobin breakdown after erythrocyte extravasation, can persist throughout the course of atherosclerotic disease. Previous studies[7,25,26] using T1-weighted sequences reported IPH resolution rates of 0%, 0%, and 6% over 17 to 18 months of follow-up. More recently, one study[9] found that IPH resolved in only 3 out of 89 scan pairs (3.4%) over an average of 1.8 years, utilizing the SNAP sequence which combines inversion-recovery gradient echo with phase-sensitive acquisition to enhance IPH-to-wall contrast and measurement accuracy[27,28]. Similarly, our study, using SNAP to detect IPH, demonstrated that all but one newly developed IPH persisted to the study end, around half arteries with pre-existing IPH continued to exhibit it throughout the study period, and hyperintense IPH signals may be observed for as long as six years. This persistence may be explained by ongoing erythrocyte extravasation from leaky neo-vessels[29].

IPH is widely recognized as a strong indicator of carotid plaque vulnerability, with its presence linked to an increased risk of future ischemic cerebrovascular events[30], independent of symptom status[31] or degree of stenosis[5,32]. In our study, despite more than half of subjects exhibited IPH at some point during follow-up, the incidence of ischemic symptoms over at least five years was low. Histological studies[29,33] have supported this observation by identifying neovasculature, a potential source of IPH, predominantly located in the adventitia away from the plaque surface, thus preserving surface integrity. This suggests that assessing plaque surface disruption[34,35] could be an important additional metric for stratifying stroke risk, particularly in asymptomatic patients. Nonetheless, IPH has been consistently associated with a rapid increase in plaque burden[7,9], and our findings added to the body of evidence by further highlighting the sustained and long-term impact of IPH presence and volume on the progression of atherosclerotic disease. Statin therapy improves cardiovascular outcomes and has demonstrated plaque regression[36–38] in multiple imaging studies, by the mechanism of modulating inflammation and decreasing or even depleting the lipid content within plaques[39–42]. However, the recent AIM-HIGH MRI sub-study[42] showed that, despite two years of intensive lipid-lowering therapy, carotid arteries with IPH experienced larger increases in lipid core size and greater reductions in lumen area compared to plaques without hemorrhage, which exhibited stabilized plaque burden and significant reductions in lipid content. This suggests the IPH's interplay with a potential non-lipid-driven pathway of plaque progression. One study[43] identified CD163+ macrophages, induced by IPH, as potential contributors to a positive feedback loop involving increased vascular permeability, inflammation, and further IPH increase. Our findings similarly highlighted the role of IPH in counteracting the systemic stabilizing effects of contemporary medical treatment. While non-IPH plaques remained stable, current therapies may be insufficient to prevent IPH-associated plaque burden

increase. Further investigation into the mechanisms behind this non-lipid-driven pathway is essential and could pave the way for novel therapeutic approaches specifically targeting IPH. Overall, there remains a significant gap in longitudinal imaging studies investigating the pathophysiology of carotid atherosclerosis and IPH, as most studies are either short-term[7,9,44] or involve long-term clinical follow-up without repeated imaging[31,45]. To the best of our knowledge, the longest imaging follow-up duration reported is 54 months[6]. However, this study was limited by a very small sample size and the use of 2D VWI, which provided inadequate coverage of the carotid bifurcation. This limitation was further compounded by challenges in identifying consistent imaging coverage for bilateral arteries and comparing multiple time points. Indeed, Geleri et al. reported that, when using the large-coverage 3D VWI sequence MERGE, only 54% of lesions were fully covered and 25% partially covered by 2D VWI in their analysis of 381 advanced plaques from the CARE-II study[46]. Recognizing these limitations, our study utilized MERGE, which provided adequate imaging coverage for bilateral and longitudinal analysis.

The emergence of deep learning-based imaging analysis also offers a promising solution to the labor-intensive nature of longitudinal VWI studies, reducing the need for extensive reviewer training and minimizing bias, as well-validated deep learning tools provide consistent and reproducible analyses across time points. While significant efforts have been made in segmenting the vessel wall on VWI[10–12], robust algorithms for detailed plaque composition segmentation remain underdeveloped[47]. In our study, we successfully utilized deep learning to integrate multi-contrast VWI, demonstrating its potential to deliver more detailed and comprehensive assessments of plaque morphology and composition[48].

Our study has a few limitations. First, although each patient underwent an average of five scans, the requirement to analyze the long-term evolution of atherosclerosis over more than five years

restricted the number of participants in this retrospective analysis. Second, the retrospective nature of this analysis resulted in a relatively healthy and stabilized patient cohort, as individuals with severe symptoms—indicative of plaques experiencing dramatic reductions in stability—were more likely to drop out of the prospective cohort early. Third, despite extensive follow-up, the absolute number of newly detected or resolved hemorrhages remained relatively low, underscoring the need for larger studies to better understand these potentially course-altering events in the plaque natural history. Finally, future research should aim to develop more advanced deep learning algorithms capable of simultaneously segmenting additional plaque components, such as lipid contents and calcification[49], to further elucidate the complex interplay between these plaque components and the pathobiology of atherosclerosis.

Conclusion

By leveraging deep learning-based segmentation on multi-contrast VWI, we successfully monitored long-term plaque dynamics across an average of five scans over a follow-up of six years in an asymptomatic cohort. Around half of the arteries with pre-existing IPH continued to exhibit it throughout the study period, while newly developed IPH also persisted, yet caused few new ischemic symptoms. Importantly, IPH disrupted the systemic symmetry of bilateral plaque progression: arteries without IPH demonstrated minimal growth under contemporary medical treatment, whereas the occurrence and volume of IPH were strongly associated with accelerated plaque burden progression.

Perspectives

Competency in medical knowledge: Demonstrates advanced knowledge of carotid atherosclerosis pathophysiology by leveraging deep learning-based segmentation on multi-contrast VWI to reveal that IPH disrupts bilateral plaque symmetry, persists over time, and significantly accelerates plaque burden progression, even under contemporary medical treatment.

Competency in patient care: Emphasizes the importance of early detection of IPH using advanced imaging techniques and advocates for personalized management strategies to mitigate its impact on plaque progression and stroke risk.

Translational outlook: The present study advocates the adoption of longitudinal patient monitoring and the integration of deep learning-based imaging tools into clinical practice to enable early assessment of plaque burden and IPH, while advancing the development of IPH-targeted therapeutics to improve patient outcomes in carotid atherosclerosis.

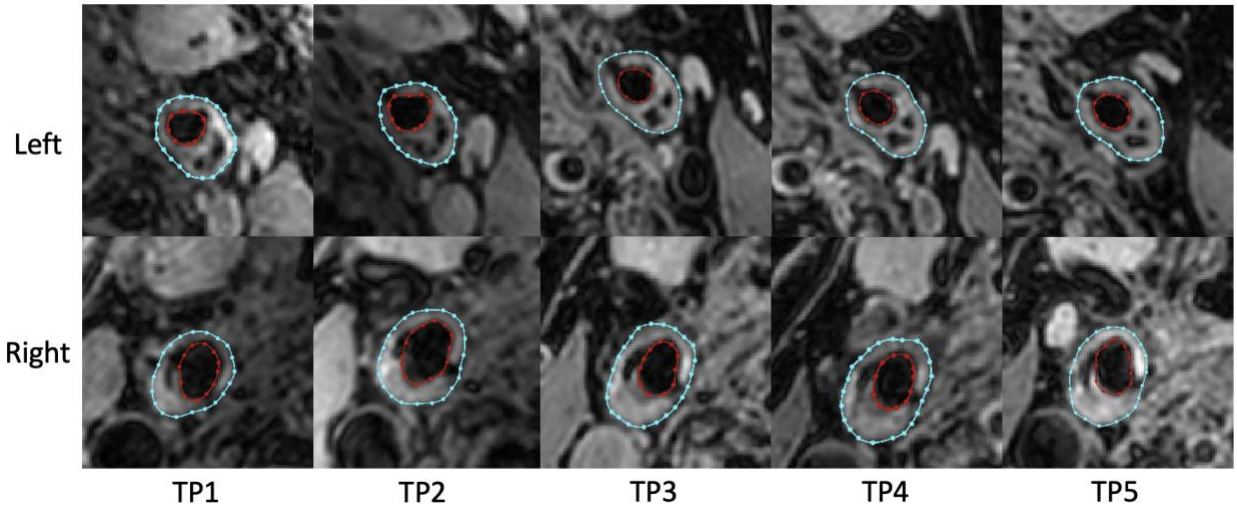

Figure 1. Example of bilateral plaque burden increases over five vessel wall imaging sessions spanning five years, demonstrating symmetrical plaque progression on both the left and right sides. The vessel wall contours were generated using deep learning-based segmentation, with red contours delineating the vessel lumen and blue contours delineating the vessel outer wall boundary. 'TP' denotes 'time point'.

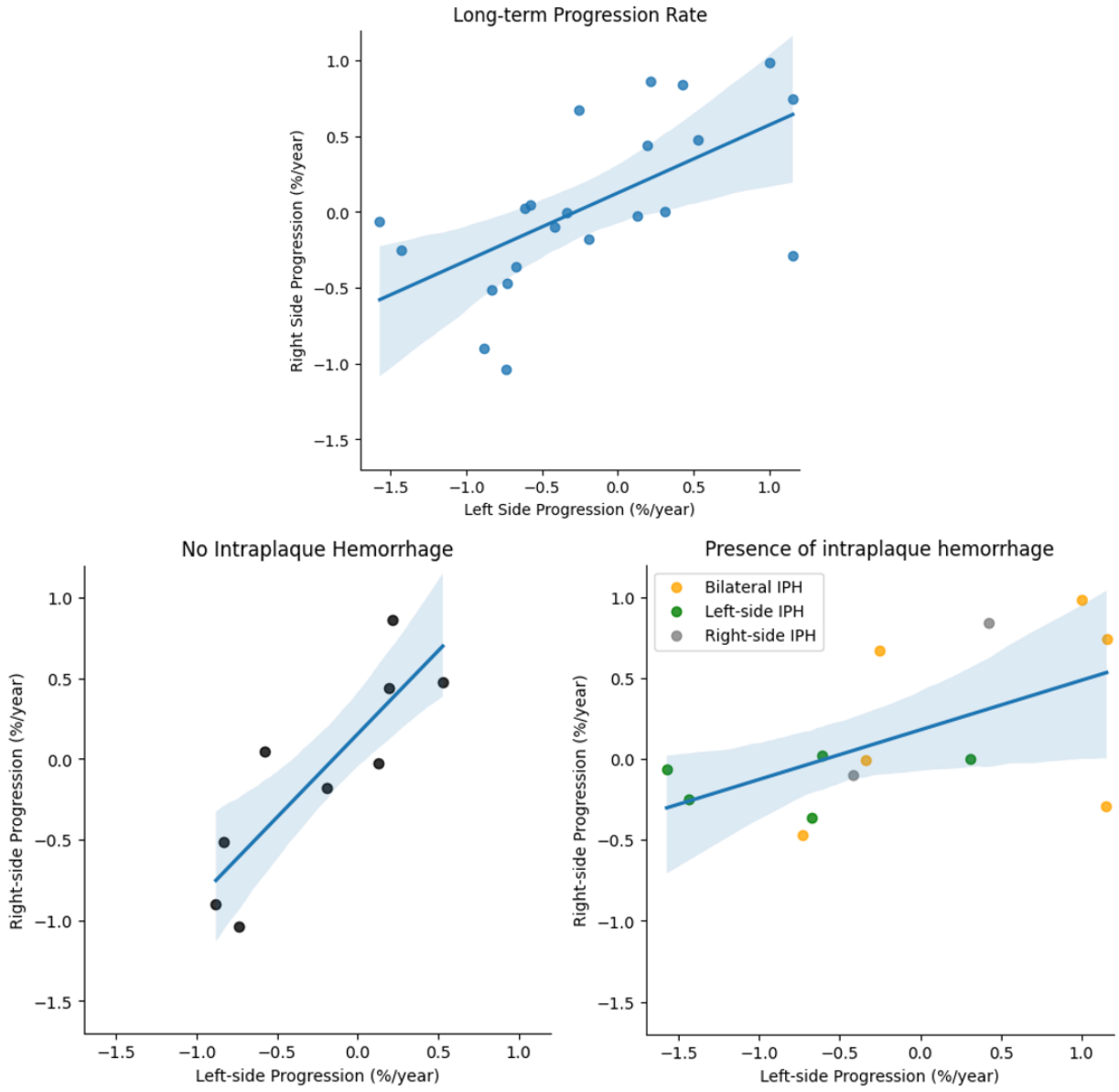

Figure 2. Upper panel: Associations of long-term growth rate of plaque burden between bilateral carotid arteries. Lower panel: Correlation of bilateral long-term progression in the two subgroups of carotid arteries with (right) and without IPH (left).

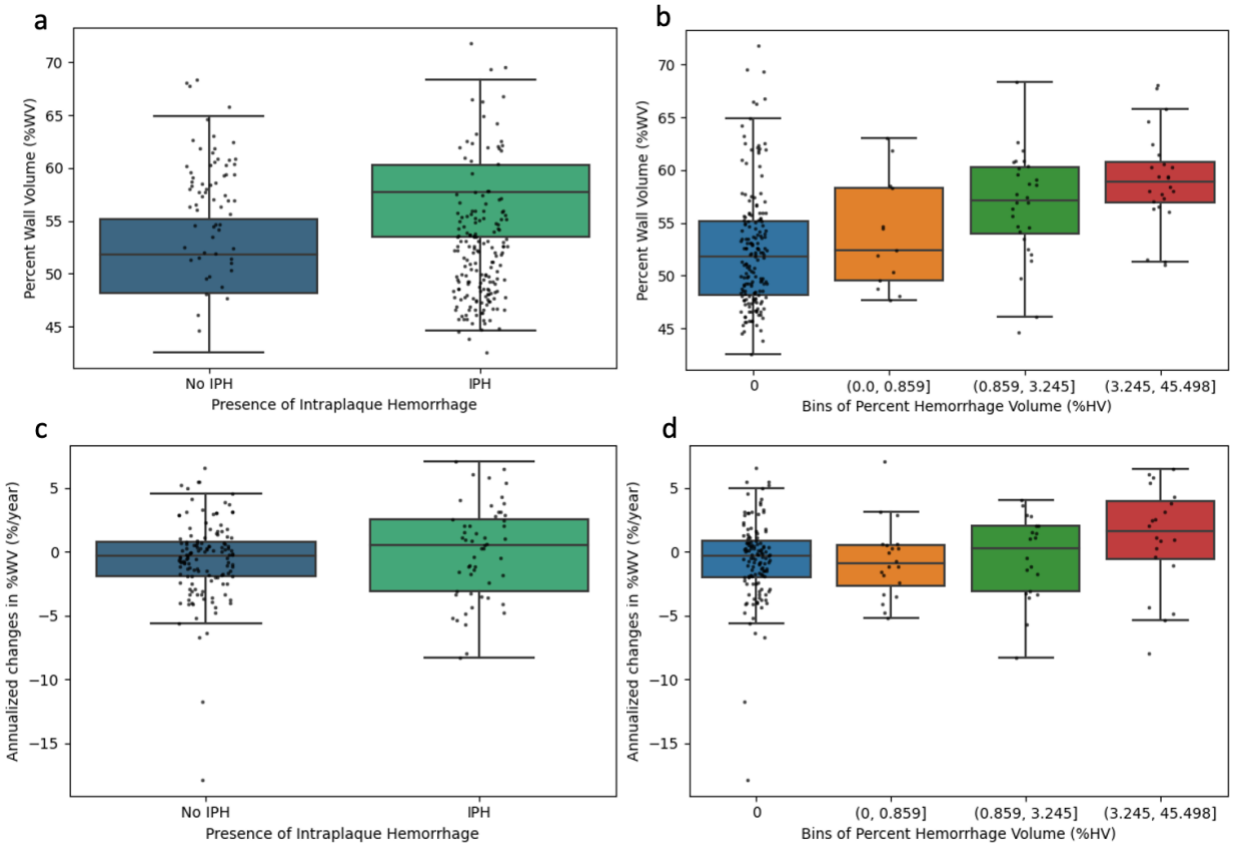

Figure 3. Box plots demonstrating the effects of presence and volume of IPH on plaque burden. In (a) and (c), %WV and annualized changes in %WV were compared based on presence or not of IPH. In (b) and (d), %HV was divided into three equal-sized bins, comparing %WV and annualized changes in %WV across different degrees of IPH volume.

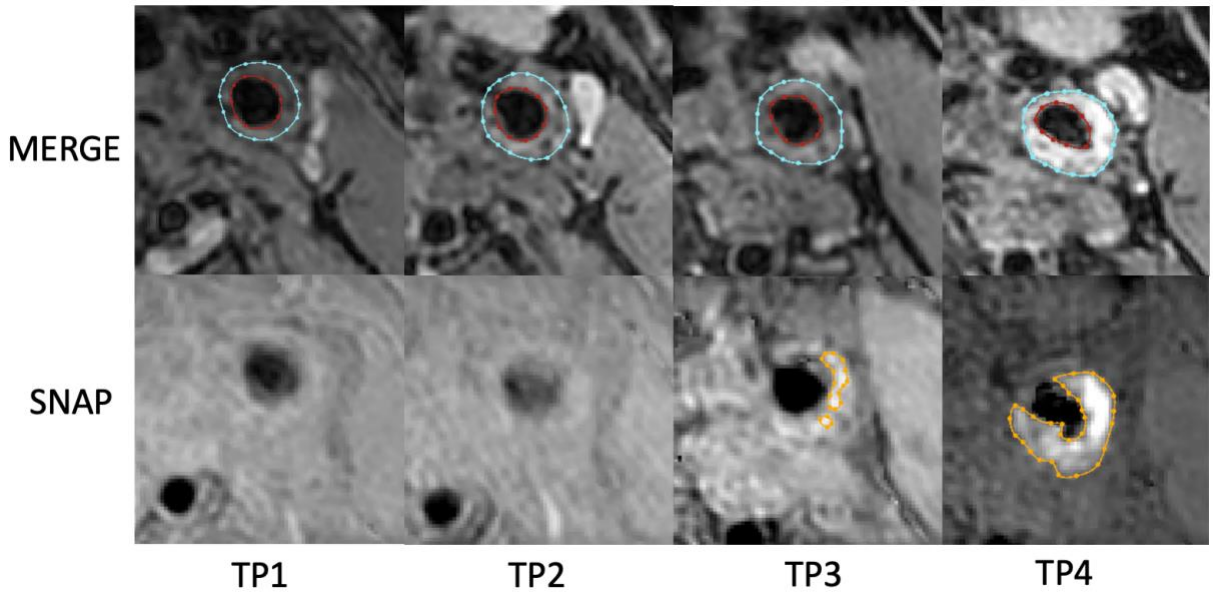

Figure 4. Example of plaque progression over four vessel wall imaging sessions spanning five years, demonstrating an increase in plaque burden, marked by the occurrence of intraplaque hemorrhage (IPH) at TP3 and subsequent volume expansion at TP4. The vessel wall and IPH contours were generated using deep learning-based segmentation, with red and blue contours delineating the vessel lumen and vessel outer wall boundary on MERGE, and orange contours delineating IPH boundary on SNAP. 'TP' denotes 'time point'.

Table 1 Population demographics at baseline

Variable	Value
Age	71.3 ± 9.7
Male sex	20 (71%)
Current smoker	3 (10%)
History of hypertension	17 (60%)
History of hyperlipidemia	25 (89%)
History of diabetes	3 (10%)
Statins	21 (75%)
Antihypertensives	16 (57%)
Antiplatelets	21 (75%)

Values are no. (%) or mean ± standard deviation

References:

1. Martin SS, Aday AW, Almarzooq ZI, et al. 2024 Heart Disease and Stroke Statistics: A Report of US and Global Data From the American Heart Association. *Circulation*. 2024;149:e347–e913.

2. Cheng SF, Brown MM, Simister RJ, Richards T. Contemporary prevalence of carotid stenosis in patients presenting with ischaemic stroke. *British Journal of Surgery*. 2019;106:872–878.

3. Mortimer R, Nachiappan S, Howlett DC. Carotid artery stenosis screening: where are we now? *British Journal of Radiology*. 2018;91:20170380.

4. Zhao X, Hippe DS, Li R, et al. Prevalence and Characteristics of Carotid Artery High-Risk Atherosclerotic Plaques in Chinese Patients With Cerebrovascular Symptoms: A Chinese Atherosclerosis Risk Evaluation II Study. *Journal of the American Heart Association*. 6:e005831.

5. Schindler A, Schinner R, Altaf N, et al. Prediction of Stroke Risk by Detection of Hemorrhage in Carotid Plaques: Meta-Analysis of Individual Patient Data. *JACC: Cardiovascular Imaging*. 2020;13:395–406.

6. Sun J, Underhill HR, Hippe DS, Xue Y, Yuan C, Hatsukami TS. Sustained Acceleration in Carotid Atherosclerotic Plaque Progression With Intraplaque Hemorrhage: A Long-Term Time Course Study. *JACC: Cardiovascular Imaging*. 2012;5:798–804.

7. Takaya N, Yuan C, Chu B, et al. Presence of Intraplaque Hemorrhage Stimulates Progression of Carotid Atherosclerotic Plaques. *Circulation*. 2005;111:2768–2775.

8. Simpson RJ, Akwei S, Hosseini AA, MacSweeney ST, Auer DP, Altaf N. MR Imaging–Detected Carotid Plaque Hemorrhage Is Stable for 2 Years and a Marker for Stenosis Progression. *American Journal of Neuroradiology*. 2015;36:1171–1175.

9. Canton G, Baylam Geleri D, Hippe DS, et al. Pathophysiology of carotid atherosclerosis: Calcification, intraplaque haemorrhage and pulse pressure as key players. *European Journal of Radiology*. 2024;178:111647.

10. Chen L, Sun J, Canton G, et al. Automated Artery Localization and Vessel Wall Segmentation Using Tracklet Refinement and Polar Conversion. *IEEE Access*. 2020;8:217603–217614.

11. Chen L, Zhao H, Jiang H, et al. Domain adaptive and fully automated carotid artery atherosclerotic lesion detection using an artificial intelligence approach (LATTE) on 3D MRI. *Magnetic Resonance in Medicine*. 2021;86:1662–1673.

12. Li X, Ouyang X, Zhang J, et al. Carotid Vessel Wall Segmentation Through Domain Aligner, Topological Learning, and Segment Anything Model for Sparse Annotation in MR Images. *IEEE Transactions on Medical Imaging*. 2024:1–1.

13. Balu N, Yarnykh VL, Chu B, Wang J, Hatsukami T, Yuan C. Carotid plaque assessment using fast 3D isotropic resolution black-blood MRI. *Magnetic Resonance in Medicine*. 2011;65:627–637.

14. Wang J, Börnert P, Zhao H, et al. Simultaneous noncontrast angiography and intraPlaque hemorrhage (SNAP) imaging for carotid atherosclerotic disease evaluation. *Magnetic Resonance in Medicine*. 2013;69:337–345.

15. Sun J, Canton G, Balu N, et al. Blood Pressure Is a Major Modifiable Risk Factor Implicated in Pathogenesis of Intraplaque Hemorrhage. *Arteriosclerosis, Thrombosis, and Vascular Biology*. 2016;36:743–749.

16. HashemizadehKolowri S, Zanaty, Nadin, Canton, Gador, Balu, Niranjan, Hatsukami, Thomas S., Yuan, Chun. Automated Localization of the Extracranial Carotid Artery in Black Blood Contrast MR Images Using a Deep Learning Approach. In: *Proc. Intl. Soc. Mag. Reson. Med*., 2023:3068.

17. Isensee F, Jaeger PF, Kohl SAA, Petersen J, Maier-Hein KH. nnU-Net: a self-configuring method for deep learning-based biomedical image segmentation. *Nat Methods*. 2021;18:203–211.

18. Guo Y, Akcicek EY, Hippe DS, et al. Abstract TP143: Longitudinal Evaluation of Vessel Wall MRI Demonstrates Bilaterally Symmetric Evolution of Carotid Atherosclerosis. *Stroke*. 2024;55:ATP143–ATP143.

19. Adams GJ, Simoni DM, Bordelon CB, et al. Bilateral Symmetry of Human Carotid Artery Atherosclerosis. *Stroke*. 2002;33:2575–2580.

20. Howard G, Burke GL, Evans GW, et al. Relations of intimal-medial thickness among sites within the carotid artery as evaluated by B-mode ultrasound. ARIC Investigators. Atherosclerosis Risk in Communities. *Stroke*. 1994;25:1581–1587.

21. Li F, Wang X. Bilateral symmetry of human carotid artery atherosclerosis: a multi-contrast weighted MR study. *Int J Cardiovasc Imaging*. 2016;32:1219–1226.

22. Shen R, Tong X, Li D, et al. Slice-based and time-specific hemodynamic measurements discriminate carotid artery vulnerable atherosclerotic plaques. *Computer Methods and Programs in Biomedicine*. 2022;225:107050.

23. Sun J, Song Y, Chen H, et al. Adventitial Perfusion and Intraplaque Hemorrhage. *Stroke*. 2013;44:1031–1036.

24. Selwaness M, van den Bouwhuijsen QJA, Verwoert GC, et al. Blood Pressure Parameters and Carotid Intraplaque Hemorrhage as Measured by Magnetic Resonance Imaging. *Hypertension*. 2013;61:76–81.

25. Underhill HR, Yuan C, Yarnykh VL, et al. Arterial Remodeling in the Subclinical Carotid Artery Disease. *JACC: Cardiovascular Imaging*. 2009;2:1381–1389.

26. van den Bouwhuijsen QJA, Selwaness M, Tang H, et al. Change in Carotid Intraplaque Hemorrhage in Community-dwelling Subjects: A Follow-up Study Using Serial MR Imaging. *Radiology*. 2017;282:526–533.

27. Ota H, Yarnykh VL, Ferguson MS, et al. Carotid Intraplaque Hemorrhage Imaging at 3.0-T MR Imaging: Comparison of the Diagnostic Performance of Three T1-weighted Sequences. *Radiology*. 2010;254:551–563.

28. Li D, Qiao H, Han Y, et al. Histological validation of simultaneous non-contrast angiography and intraplaque hemorrhage imaging (SNAP) for characterizing carotid intraplaque hemorrhage. *Eur Radiol*. 2021;31:3106–3115.

29. Virmani R, Kolodgie FD, Burke AP, et al. Atherosclerotic Plaque Progression and Vulnerability to Rupture. *Arteriosclerosis, Thrombosis, and Vascular Biology*. 2005;25:2054–2061.

30. Gupta A, Baradaran H, Schweitzer AD, et al. Carotid Plaque MRI and Stroke Risk. *Stroke*. 2013;44:3071–3077.

31. Takaya N, Yuan C, Chu B, et al. Association Between Carotid Plaque Characteristics and Subsequent Ischemic Cerebrovascular Events. *Stroke*. 2006;37:818–823.

32. Saam T, Hetterich H, Hoffmann V, et al. Meta-Analysis and Systematic Review of the Predictive Value of Carotid Plaque Hemorrhage on Cerebrovascular Events by Magnetic Resonance Imaging. *Journal of the American College of Cardiology*. 2013;62:1081–1091.

33. Sluimer JC, Kolodgie FD, Bijnens APJJ, et al. Thin-Walled Microvessels in Human Coronary Atherosclerotic Plaques Show Incomplete Endothelial Junctions: Relevance of Compromised Structural Integrity for Intraplaque Microvascular Leakage. *Journal of the American College of Cardiology*. 2009;53:1517–1527.

34. Ota H, Yu W, Underhill HR, et al. Hemorrhage and Large Lipid-Rich Necrotic Cores Are Independently Associated With Thin or Ruptured Fibrous Caps. *Arteriosclerosis, Thrombosis, and Vascular Biology*. 2009;29:1696–1701.

35. Chen S, Zhao H, Li J, et al. Evaluation of carotid atherosclerotic plaque surface characteristics utilizing simultaneous noncontrast angiography and intraplaque hemorrhage (SNAP) technique. *Journal of Magnetic Resonance Imaging*. 2018;47:634–639.

36. Corti R, Worthley SG, Helft G, et al. Effects of Aggressive Versus Conventional Lipid-Lowering Therapy by Simvastatin on Human Atherosclerotic Lesions: A Prospective, Randomized, Double-Blind Trial With High-Resolution Magnetic Resonance Imaging. *Journal of the American College of Cardiology*. 2005;46:106–112.

37. Underhill HR, Yuan C, Zhao X-Q, et al. Effect of rosuvastatin therapy on carotid plaque morphology and composition in moderately hypercholesterolemic patients: A high-resolution magnetic resonance imaging trial. *American Heart Journal*. 2008;155:584.e1-584.e8.

38. Lee JMS, Wiesmann F, Shirodaria C, et al. Early changes in arterial structure and function following statin initiation: Quantification by magnetic resonance imaging. *Atherosclerosis*. 2008;197:951–958.

39. Zhao X-Q, Dong L, Hatsukami T, et al. MR Imaging of Carotid Plaque Composition During Lipid-Lowering Therapy: A Prospective Assessment of Effect and Time Course. *JACC: Cardiovascular Imaging*. 2011;4:977–986.

40. Dong L, Kerwin WS, Chen H, et al. Carotid Artery Atherosclerosis: Effect of Intensive Lipid Therapy on the Vasa Vasorum—Evaluation by Using Dynamic Contrast-enhanced MR Imaging. *Radiology*. 2011;260:224–231.

41. Kini AS, Baber U, Kovacic JC, et al. Changes in Plaque Lipid Content After Short-Term Intensive Versus Standard Statin Therapy: The YELLOW Trial (Reduction in Yellow Plaque by Aggressive Lipid-Lowering Therapy). *Journal of the American College of Cardiology*. 2013;62:21–29.

42. Zhao X-Q, Sun J, Hippe DS, et al. Magnetic Resonance Imaging of Intraplaque Hemorrhage and Plaque Lipid Content With Continued Lipid-Lowering Therapy: Results of a Magnetic Resonance Imaging Substudy in AIM-HIGH. *Circulation: Cardiovascular Imaging*. 2022;15:e014229.

43. Guo L, Akahori H, Harari E, et al. $CD163^+$ macrophages promote angiogenesis and vascular permeability accompanied by inflammation in atherosclerosis. *J Clin Invest*. 2018;128:1106–1124.

44. Guo Y, Canton G, Baylam Geleri D, et al. Plaque Evolution and Vessel Wall Remodeling of Intracranial Arteries: A Prospective, Longitudinal Vessel Wall MRI Study. *Journal of Magnetic Resonance Imaging*. 2024;60:889–899.

45. Nies KPH, Aizaz M, van Dam-Nolen DHK, et al. Signal intensity and volume of carotid intraplaque hemorrhage on magnetic resonance imaging and the risk of ipsilateral cerebrovascular events: The Plaque At RISK (PARISK) study. *Journal of Cardiovascular Magnetic Resonance*. 2024;26:101049.

46. Baylam Geleri D, Watase H, Chu B, et al. Detection of Advanced Lesions of Atherosclerosis in Carotid Arteries Using 3-Dimensional Motion-Sensitized Driven-Equilibrium Prepared Rapid Gradient Echo (3D-MERGE) Magnetic Resonance Imaging as a Screening Tool. *Stroke*. 2022;53:194–200.

47. Guo Y, Li J, Liu D, et al. Carotid plaque composition segmentation in multi-contrast MRI with U-net. In: *Proc. Intl. Soc. Mag. Reson. Med*., 2019:2145.

48. Cai J-M, Hatsukami TS, Ferguson MS, Small R, Polissar NL, Yuan C. Classification of Human Carotid Atherosclerotic Lesions With In Vivo Multicontrast Magnetic Resonance Imaging. *Circulation*. 2002;106:1368–1373.

49. Wang X, Canton G, Guo Y, et al. Automated MRI-based segmentation of intracranial arterial calcification by restricting feature complexity. *Magnetic Resonance in Medicine*. 2025;93:384–396.

Supplementary Table S1

Section	**Checklist item**	**Guo et al.**
1	**Designing the study plan**	
1.1	Describe the need for the application of machine learning to the dataset	pg 7-8
1.2	Describe the objectives of the machine learning analysis	pg 7-8
1.3	Define the study plan	pg 7-9, suppl. pg 1-2
1.4	Describe the summary statistics of baseline data	Table 1
1.5	Describe the overall steps of machine learning workflow	pg 7-8
2	**Data standardization, feature engineering, and learning**	
2.1	Describe how the data were processed in order to make it clean, uniform, and consistent	suppl. pg 1
2.2	Describe whether variables were normalized and if so, how this was done	suppl. pg 1
2.3	Provide details on the fraction of missing values (if any) and imputation methods	N/A
2.4	Perform and describe feature selection process	N/A
2.5	Identify and describe the process to handle outliers if any	N/A
2.6	Describe whether class imbalance existed, and which method was applied to deal with it	N/A
3	**Selection of Machine Learning Model**	
3.1	Explicitly define the goal of the analysis e.g., regression, classification, clustering	pg 7-9
3.2	Identify the proper learning method used (e.g., supervised, reinforcement learning etc.) to address the problem	pg 7-8
3.3	Provide explicit details on the use of simpler, complex, or ensemble models	pg 7-8
3.4	Provide the comparison of complex models against simpler models if possible	N/A
3.5	Define ensemble methods, if used	N/A
3.6	Provide details on whether the model is interpretable	N/A
4	**Model Assessment**	
4.1	Provide a clear description of data used for training, validation, and testing	pg 7
4.2	Describe how the model parameters were optimized (e.g., optimization technique, number of model parameters etc.)	pg 7
5	**Model Evaluation**	
5.1	Provide the metric(s) used to evaluate the performance of the model	suppl. pg 1-2
5.2	Define the prevalence of disease and the choice of the scoring rule used	pg 10, suppl. pg 1
5.3	Report any methods used to balance the numbers of subjects in each class	N/A
5.4	Discuss the risk associated to misclassification	N/A
6	**Best Practices for Model Replicability**	

6.1	Consider sharing code or scripts on public repository with appropriate copyright protection steps for further development and non-commercial use	X
6.2	Release data dictionary with appropriate explanation of the variables	X
6.3	Document version of all software and external libraries	X
7	**Reporting limitations, biases and alternatives**	
7.1	Identify and report the relevant model assumptions and findings	suppl. pg 2-3
7.2	If well performing models were tested on a hold-out validation dataset, detail the data of that validation set with the same rigor as that of training dataset (see section 2 above)	suppl. pg 1